Journal of Power Sources 237 (2013) 285–290

Contents lists available at SciVerse ScienceDirect

Journal of Power Sources

journal homepage: www.elsevier.com/locate/jpowsour

Investigation on gas generation of $Li_4Ti_5O_{12}$/$LiNi_{1/3}Co_{1/3}Mn_{1/3}O_2$ cells at elevated temperature

Kai Wu [a,c], Jun Yang [a,*], Yang Liu [b], Yao Zhang [c], Chenyun Wang [b], Jinmei Xu [c], Feng Ning [c], Deyu Wang [b,**]

[a] School of Chemistry and Chemical Engineering, Shanghai Jiao Tong University, 800 Dongchuan Road, Shanghai 200240, PR China
[b] Ningbo Institute of Material Technology and Engineering, Chinese Academy of Science, 509 Zhuangshi Road, Zhenhai, Ningbo 315201, PR China
[c] Amperex Technology Limited, 1 West Industrial Road, North Zone of SSL Sci. & Tech. Industry Park, Dongguan 523808, PR China

HIGHLIGHTS

- The key factors of gassing in $Li_4Ti_5O_{12}$ cells are investigated by the accelerating measurement.
- The chemically catalytic reaction related to moisture makes a minor contribution to $Li_4Ti_5O_{12}$ cell gassing.
- Graphite cells show a similar swelling behavior at over-discharge state as $Li_4Ti_5O_{12}$ cells.
- Electrolyte decomposition at elevated temperature should be dominated by the anode potential.

ARTICLE INFO

Article history:
Received 13 January 2013
Received in revised form
8 March 2013
Accepted 12 March 2013
Available online 21 March 2013

Keywords:
Lithium ion battery
Lithium titanate
Cell swelling
Elevated temperature

ABSTRACT

The possible reasons and key factors on gas generation of $Li_4Ti_5O_{12}$ (LTO) cells are investigated by the accelerating measurement baking at 80 °C for 120 h. It is found that the chemically catalytic reaction related to moisture makes a minor contribution to cell swelling. Our LTO-based 383450 cells (~10 mL) before pre-charge (i.e. formation) only produce ~1.5 mL gas during baking test and CO_2, instead of H_2, is the dominant species in EC/DMC electrolyte. By contrast, the swelling ratio of the charged LTO cells, which are re-sealed after formation, is kept at ~97% regardless of states of charge. This severe decomposition of carbonates at elevated temperature should be dominated by the anode potential, rather than catalysis of LTO, since graphite/NMC cells show a similar swelling behavior at over-discharge state, where graphite anode shares the same potential as LTO. On the other hand, the electrolyte stability is also dependent on the type of solvent. Among the investigated systems, the mixture of PC + DMC (1:1) exhibits the best behavior to suppress the cell swelling. The swelling ratio diminishes from ~100% of other electrolytes to 50%. This improvement probably roots in the high quality of protective films formed during solvents' decomposition.

1. Introduction

Recently, lithium ion batteries have drawn tremendous attention due to the potential application in electric vehicles and smart grid. Lithium titanate ($Li_4Ti_5O_{12}$, LTO), which was firstly proposed by J.R. Dahn et al. [1,2], is regarded as one of the most attractive anode materials for an ultra-long life lithium ion battery owing to its zero volumetric variation [3,4] and absence of SEI reformation. In addition, this material presented better rate capability in low temperature than graphite as a result of the lower de-solvation energy of Li^+-solvents complex on its surface [5]. Therefore, lithium ion batteries with LTO anode have been proposed as one of the most attractive power batteries used in HEV [6–8].

However, batteries with LTO anode are still not widely used due to the unexpected swelling at elevated temperature, which seriously deteriorated its power density and cyclic stability [9,10]. In our previous work, it was recognized that gases were produced from LTO side and H_2 gas was the extra-dominant species [9]. Recently, He Y.B. et al. studied gassing behavior of LTO battery at room temperature and showed that carbon coated LTO did not cause considerable cell swelling after stored for 3 months or cycled 400 times at room temperature [11]. However, our previous work brought forward that gas generation of LTO battery at elevated temperature must be eliminated and storage at 80 °C for 120 h could be a good accelerating measurement for LTO battery based on our accelerated storage model in view of that its potential HEV and

* Corresponding author. Tel.: +86 21 54747667; fax: +86 21 54741297.
** Corresponding author. Tel.: +86 574 86688084; fax: +86 574 86685043.
E-mail addresses: yangj723@sjtu.edu.cn (J. Yang), wangdy@nimte.ac.cn (D. Wang).

0378-7753/$ – see front matter © 2013 Elsevier B.V. All rights reserved.
http://dx.doi.org/10.1016/j.jpowsour.2013.03.057

energy storage applications require more than 10 years of service life [9]. To the best of our knowledge, gas generation behavior of LTO battery at elevated temperature has not been fully understood and associated decomposition mechanism of solvents is not very clear yet. In this paper, the inherent reason of gas generation at elevated temperature and the key influencing factors are intensively investigated. The possible mechanisms of carbonates' decomposition are revealed based on cell gases and remnants on LTO electrodes.

2. Experiments

Spinel $Li_4Ti_5O_{12}$ was synthesized by a solid-state route. Stoichiometric amounts of Li_2CO_3 (Chinese Lithium Com., 99.9%) and TiO_2 (99%, Pule Chem.) with appropriate amount of sugar were ball-milled for 4 h and sintered at 800 °C for 24 h under N_2. After cooled down to room temperature, the powder was pulverized and vacuumed in Al-plastic laminate foil for storage. The home-made $Li_4Ti_5O_{12}$ coated with 1.6 wt% carbon was used as anode active material. $LiNi_{1/3}Co_{1/3}Mn_{1/3}O_2$ (NMC) and the electrolyte solvents were purchased from 3M (Shanghai, China) and Guotaihuarong (Zhangjiagang, China) respectively. The other battery materials were obtained from Amperex Technology Limited Com. (ATL).

383450-type LTO/NMC batteries were designed with a capacity of 300 mA h. Both LTO and NMC electrodes were composed of 90 wt % active materials, 5 wt% PVdF, and 5 wt% Super-P. The coating weight was controlled as 5.3 mg cm^{-2} for LTO electrode and 7.1 mg cm^{-2} for NMC. Celgard® 2500 was used as separator. The cells were assembled by a typical pouch cell manufacturing process. Before electrolyte injection, the cells were dried in a vacuum oven at 85 °C for 12 h. The moisture content of LTO electrode, NMC electrode and separator after drying were 350 ppm, 140 ppm and 110 ppm, respectively. The cells were pre-sealed after electrolyte injection, and stored for 24 h at ambient temperature to ensure good electrolyte wetting. Afterward, the cells were pre-charged (also called formation) at ambient temperature to 2.8 V followed by final vacuum sealing (−90 kPa). During vacuum sealing, extra Al-plastic laminate foil (called air bag, as shown in Fig. 1a) saved aside to accommodate possible gases generated during high temperature baking. Unless specified otherwise, the cells after final vacuum sealing were cycled twice between 1.5 V and 2.8 V to stabilize the cell chemistry and measure capacity prior to high temperature storage. The finished cells were at fully charge state (100% SOC).

383450-type Graphite/NMC batteries were also assembled for a comparison. Graphite electrode was made of 96% graphite, 2% PVdF and 2% Super P. The composition and dimension of NMC electrode were the same as those of LTO batteries. The coating weights of graphite and NMC electrode were 4.9 mg cm^{-2} and 10.2 mg cm^{-2} respectively. The other materials and manufacturing processes were the same as LTO/NMC batteries but the pre-charge cut-off voltage was controlled at 3.80 V before final vacuum sealing.

To measure anode (graphite or LTO) potential vs. Li/Li^+ related to different SOC of cells during charging and discharging, the 3-electrode cells were fabricated by inserting enameled copper wire (20 μm in diameter) between cathode and anode electrode of cell Jelly-roll during cell assembly. The insulating material of enameled copper wire tip (approximately 5 mm long) was removed by high concentration sulfuric acid (98.3 wt%) followed by rinsing three times with DI water/acetone and drying before cell assembly. The exposed 5 mm tip of enameled copper wire was electrically insulated from both cathode and anode electrode with an extra piece of separator during cell assembly. These 3-electrode cells were activated by electrochemical Li-plating onto exposed Cu wire tip from NMC cathode.

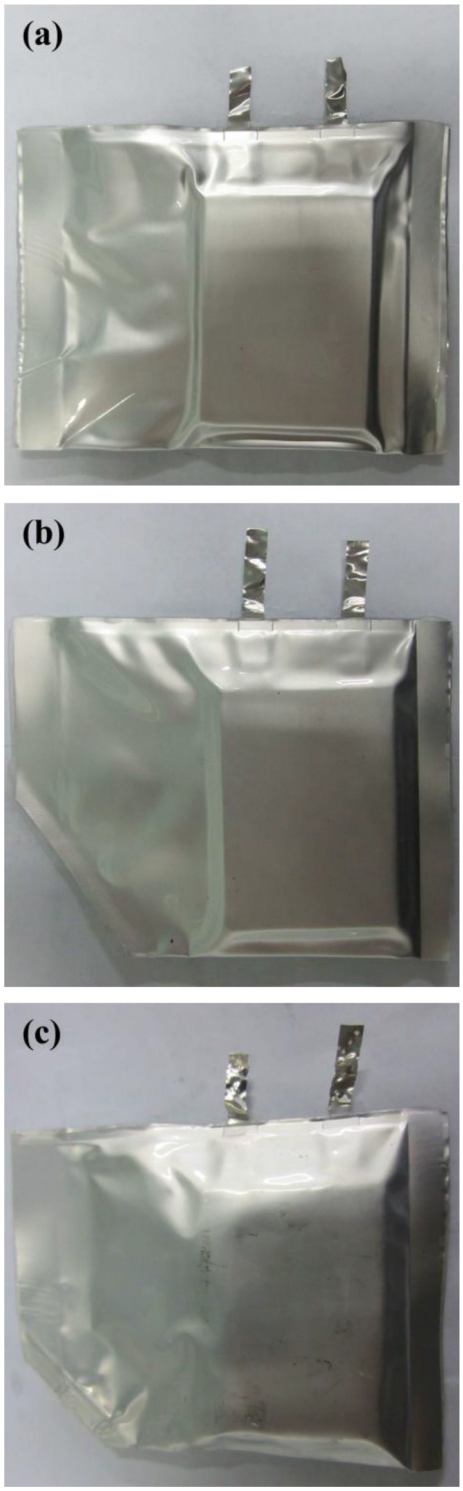

Fig. 1. Digital pictures of LTO/NMC cells. a: Before electrolyte injection; b: after formation; c: after baking.

The electrolytes were 1 mol L^{-1} $LiPF_6$ in the solvents of dimethyl carbonate (DMC), diethyl carbonate (DEC), methyl ethyl carbonate (EMC), propylene carbonate (PC), ethylene carbonate (EC) + DMC (1:1, w/w), PC + DMC (1:1, w/w), and PC + DEC (1:1, w/w). Lithiated molecular sieve was used to remove moisture of electrolyte solvents. H_2O content of as-prepared electrolyte was found to be 15 ppm by Karl-Fisher titration. After drying cells at 85 °C for 12 h in

vacuum chamber, 3.3 g electrolyte was injected into the cells. The aforementioned operations were conducted in a M-Braun glove box as oxygen and moisture was controlled less than 1 ppm, and a big chamber was equipped with an oven.

Baking experiments at 80 °C for 120 h were performed in a temperature-controlled oven. To calculate the swelling ratio, the volume of cells was measured after electrolyte injection, after formation and after baking by utilizing water draining method. The cell's volume after baking was measured after cooling at room temperature for 6 h. Fig. 1b and c shows the typical digital photos of the LTO cell after formation and after baking. For the convenience of discussion, the volume of generated gas calibrated as 383450 cells is 10 ml.

To investigate the influence of water content, various amounts of DI water were injected into 3.3 g electrolyte of 1 mol L^{-1} $LiPF_6$ in EC + DMC, and sealed in the Al-plastic laminate foil bags. The electrolyte bags were baked at 80 °C for 120 h. The swelling ratio was measured by the aforementioned water draining method.

X-ray diffraction (XRD) measurement was carried out with a D8-Brucker diffractometer equipped with Cu Kα radiation. Surface analysis was conducted with a PHI 3056 X-ray photoelectron spectrometer (XPS) which was excited by a Mg Kα radiation at a constant power of 100 W (15 kV and 6.67 mA). A QUANTA FEC-250 scanning electron microscope (SEM) was used to image the LTO electrode after baking. Gas-chromatography (GC) was conducted in a PC controlled Agilent 7890A to analyze the gas compositions in batteries. Aqueous content was analyzed with KF831/832 Karl Fisher Coulometer. Infrared measurements were conducted with Nicolet 6700FTIR scanned between 400 and 4000 cm^{-1}.

Before electrode analysis, the cells were carefully disassembled, rinsed with dimethyl carbonate (DMC) in an argon-filled glove box, and then vacuum-dried in small chamber of glove-box overnight. The samples for Infrared (IR) spectrum, Scanning Electron Microscope (SEM), X-ray Photo-electron Spectrum (XPS) and X-ray diffraction (XRD) characterizations were prepared in an Ar-filled glove box (moisture and O_2 content less than 1 ppm) and transported to the characterization equipments via an air-proof bottle to avoid ambient air/moisture contamination.

3. Results and discussion

3.1. Influence of water content

The moisture in graphite electrode could be eliminated during formation since the reduction of water was peaked at 1.2 V vs. Li/Li^+ [12]. However, large part of the absorbed moisture in LTO electrode remains intact after formation because its working potential is above 1.3 V vs. Li/Li^+. The remained moisture will chemically react with PF_6^- to form POF_3, which can catalyze the carbonate solvents decomposing to various species, including CO_2 gas [13].

To investigate the influence of water content, a given amount of deionic water was directly injected into 3.3 g electrolyte of 1 mol L^{-1} $LiPF_6$ in EC + DMC separately to reach the water content of 200, 500, 1000, 2000, 10,000 and 20,000 ppm respectively. Table 1 shows the gas volume after baking experiments with different water content. The pristine electrolyte, which contained 15 ppm H_2O, generated 0.5 mL gas, corresponding to 5% swelling of full cell. When moisture content reached 200, 500 and 1000 ppm, the increased volumes of the cells were 1.6, 3.3 and 4.6 mL respectively. This swelling extent will seriously influence the cell's appearance and exert a catastrophic effect on battery performance, such as power fading and cyclic instability. When the moisture content was increased to 5000, 10,000 and 20,000 ppm, the cells expanded for more than 60%. Furthermore, CO_2 gas accounted for a weight ratio of ~80% among the gaseous species, in similar to the Gachot's result [13].

Table 1
Influence of water content on cell swelling at 80 °C for 120 h.

Sample	Electrolyte (g)	Injected water (ppm)	Gas volume (ml)	Swelling ratio of full cell (%)
A	3.30	0	0.5	5
B	3.30	200	1.6	16
C	3.30	500	3.3	33
D	3.30	1000	4.6	46
E	3.30	5000	6.3	63
F	3.30	10,000	7.5	75
G	3.30	20,000	9.9	99
LTO/NMC cell before formation	3.30	0	1.5	15

Note: The cell's volume is averaged as 10 mL.

To quantify the influence of electrode moisture, the baking measurements were conducted for LTO/NMC cells before formation. The water content in electrolyte would enhance to ~344 ppm provided the moisture absorbed in LTO electrode (~350 ppm), NMC electrode (~140 ppm) and separator (~110 ppm) was totally dissolved into the electrolyte. After baking experiments, the cells only expanded around 15.6%, which is close to the result of pure electrolyte containing 200 ppm injected water. Furthermore, CO_2 was the extremely dominant gaseous species, which was the same as that in electrolyte bags. Therefore, the cell swelling before formation could be attributed to the chemical catalysis of POF_3, which was produced by the reaction of H_2O and PF_6^-. In other words, the moisture in electrodes and separator only contributed ~15.6% cell swelling in our systems.

3.2. Influence of cell's SOC

The LTO/NMC cells after vacuum re-sealing were charged to 0%, 25%, 50%, 75% and 100% of SOC, and followed by the baking tests. As shown in Fig. 2, cell's swelling ratio was kept to ~97% regardless of SOC. This expansion was ~5 times larger than that of cells before formation. The less sensitivity to SOC should be related to the flat discharge plateau of LTO anode. As for the same swelling ratio of 0% SOC, it probably indicated that enough amount of $Li_7Ti_5O_{12}$ remained on the surface to reduce carbonates. The generated gas was around 4.3×10^{-4} mol, which will consume ~8.6×10^{-4} mol Ti [III], namely 137 mg of $Li_7Ti_5O_{12}$, if two electrons were consumed to produce one molecule gas. It was possible to remain this amount of Ti [III] to react with solvents at 0% SOC.

Compared to Graphite/NMC system, LTO/NMC cells possessed the different anode material and working potential, which could be

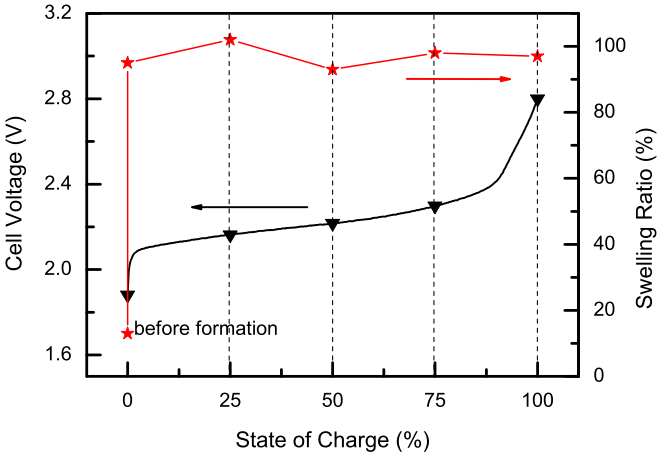

Fig. 2. Swelling ratio of LTO/NMC cells at various states of charge.

Table 2
Gas species and ratio of Graphite/NMC cells.

Cell	Potential (V)			Swelling (%)	H_2 (%)	CO (%)	CO_2 (%)	C_3H_6 (%)	C_3H_8 (%)	C_2H_4 (%)	C_2H_6 (%)	CH_4 (%)
	Cell	Cathode (vs. Li/Li^+)	Anode (vs. Li/Li^+)									
G-NMC	3.83	3.96	0.13	31	25.1	12.4	15.0	0.0	0.1	3.0	2.3	42.2
	3.26	3.51	0.25	95	78.5	0.7	15.5	0.1	0.0	2.2	0.4	2.5
	1.78	3.34	1.56	141	48.1	0.1	49.8	0.0	0.0	0.1	0.4	1.5
LTO/NMC	2.21	3.76	1.55	93	70.2	8.3	6.3	0.0	0.0	13.9	0.2	1.2

the reason for this severe cell swelling. To confirm the real reason for carbonates' decomposition, Graphite/NMC cells with 1 mol L^{-1} $LiPF_6$ in EC + DMC (1:1) as electrolyte were discharged to different potential and then conducted the baking experiments. As shown in Table 2, Graphite/NMC cells were also swollen after baking experiments. When graphite electrode was discharged to 0.13 V, 0.25 V and 1.56 V vs. Li/Li^+, the cells were expanded to 31%, 95% and 141% respectively. Among the gaseous species in Graphite/NMC cells, the large amount of CO_2 gas in graphite (1.56 V) cells could be related to decomposition of organic components in SEI film. It was worthy to note that the amount of H_2 gas in graphite (0.25 V and 1.56 V) cells is close to that in LTO (1.55 V) cells, 7.46 mL, 6.78 mL and 6.53 mL respectively. The considerable amount of H_2 gas in graphite cells at 1.56 V could be attributed to the loss of SEI's protection at higher potential. This result provided a direct evidence that the electrode potential is closely related to carbonates' decomposition.

3.3. Influence of solvents

To verify if carbonates have a crucial impact on swelling, DMC, DEC, EMC, PC, EC + DMC (1:1, w/w), PC + DMC (1:1, w/w), PC + DEC (1:1, w/w) were utilized as electrolyte solvents to compare their influence. As shown in Fig. 3, the cell with DMC electrolyte generated the largest amount of gas, 32.5 mL, corresponding to 325% of cell swelling. PC, EMC and DEC electrolytes produced less gas, 15.4 mL, 11.0 mL and 8.8 mL, respectively. As the mixed solvents PC + DEC and EC + DMC were used, the cells expanded for 90% and 95% respectively. The mixture of PC + DMC presented the best behavior to suppress gas generation. The cells containing this electrolyte only produced 5.0 mL gas, corresponding to 50% swelling.

Since the electrolyte with PC + DMC produced the least amount of gas, the influence of their ratio was further investigated. As shown in Fig. 4, in contrast to DMC electrolyte, the swelling ratio of LTO cell was reduced significantly after PC was added. Swelling dropped from 325% of the DMC electrolyte to 60%, 50% and 54% of the electrolytes containing 20%, 50% and 60% PC. With a further increase in PC content, the cell swelling was aggravated to 72% in 7:3, 126% in 8:2 of PC:DMC, and 154% in pure PC electrolyte. This distortional smiling-curve indicates that the mutual-effect of PC and DMC plays a critical role to diminish the amount of cell gas.

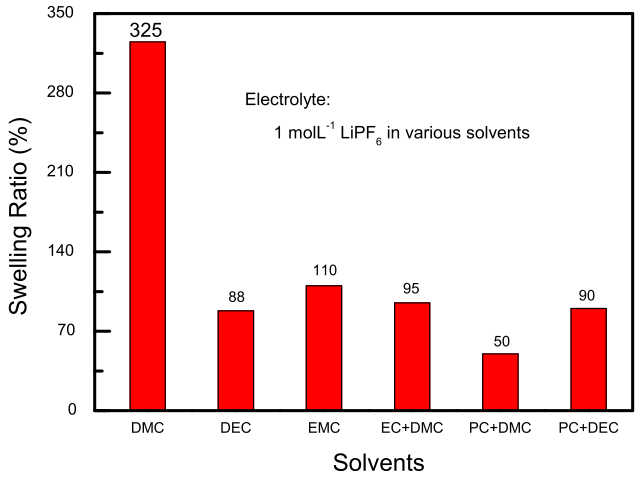

Fig. 3. Swelling ratio of LTO/NMC cells in the electrolytes of 1 mol L^{-1} $LiPF_6$ in different solvents. The ratio of mixed solvents is 1:1 by weight.

3.4. Decomposition mechanism of electrolyte solvents

To explore the decomposing process of solvents, the cell gas was analyzed with gas-chromatography (GC). As shown in Table 3, it could be concluded that CH_4 and C_3H_6 were the characteristic gas of DMC and PC respectively. C_2H_6 appeared more when DEC used, and C_2H_4 amount significantly increased in EC containing electrolyte. Although H_2 was the dominant species in most of electrolytes, C_3H_6

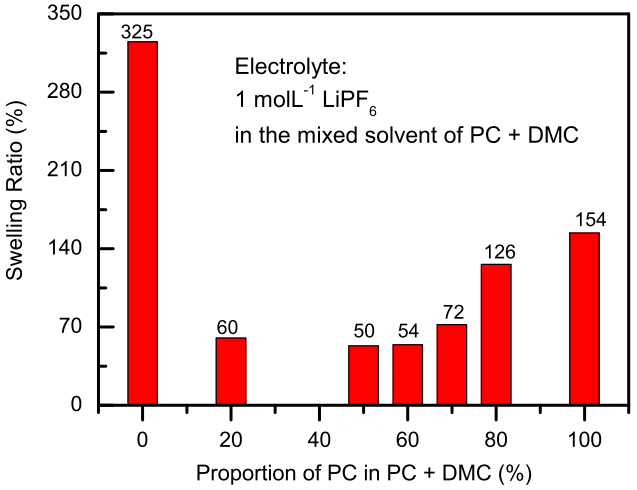

Fig. 4. Swelling ratio of LTO/NMC cells in the electrolytes of 1 mol L^{-1} $LiPF_6$ in PC + DMC at various ratio.

Table 3
Gas species and ratio of LTO/NMC cells (unit: %).

Electrolyte	Swelling	H_2	CO	CO_2	C_3H_6	C_3H_8	C_2H_4	C_2H_6	CH_4
$LiPF_6$ in DMC	325	81.5	5.3	10.1	0.0	0.0	0.0	0.0	2.9
$LiPF_6$ in DEC	88	81.0	1.8	14.2	0.0	0.0	1.1	1.8	0.0
$LiPF_6$ in EC + DMC (1:1)	95	70.2	8.3	6.3	0.0	0.0	13.9	0.2	1.2
$LiPF_6$ in PC + DMC (1:1)	50	74.6	10.8	3.1	9.4	0.0	0.1	0.0	2.1
$LiPF_6$ in PC + DEC (1:1)	90	74.7	7.7	4.0	12.4	0.0	0.1	1.1	0.1
$LiPF_6$ in PC + DMC (4:1)	126	9.3	11.0	1.1	77.2	0.0	0.1	0.1	1.3
$LiPF_6$ in PC + DEC (4:1)	135	7.2	12.7	19.2	59.0	0.0	0.2	1.7	0.1

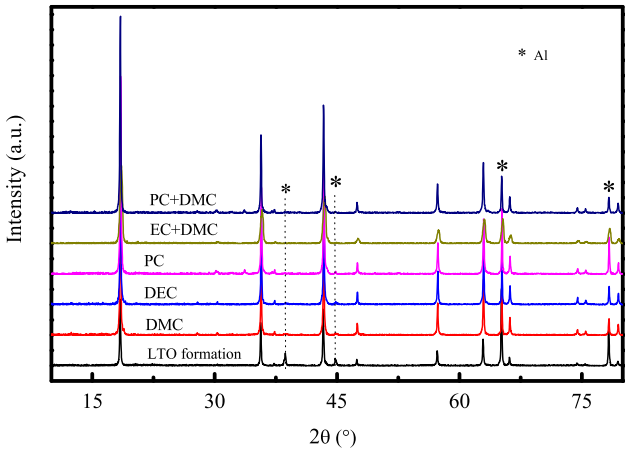

Fig. 5. XRD patterns of LTO electrodes after baking in different electrolytes.

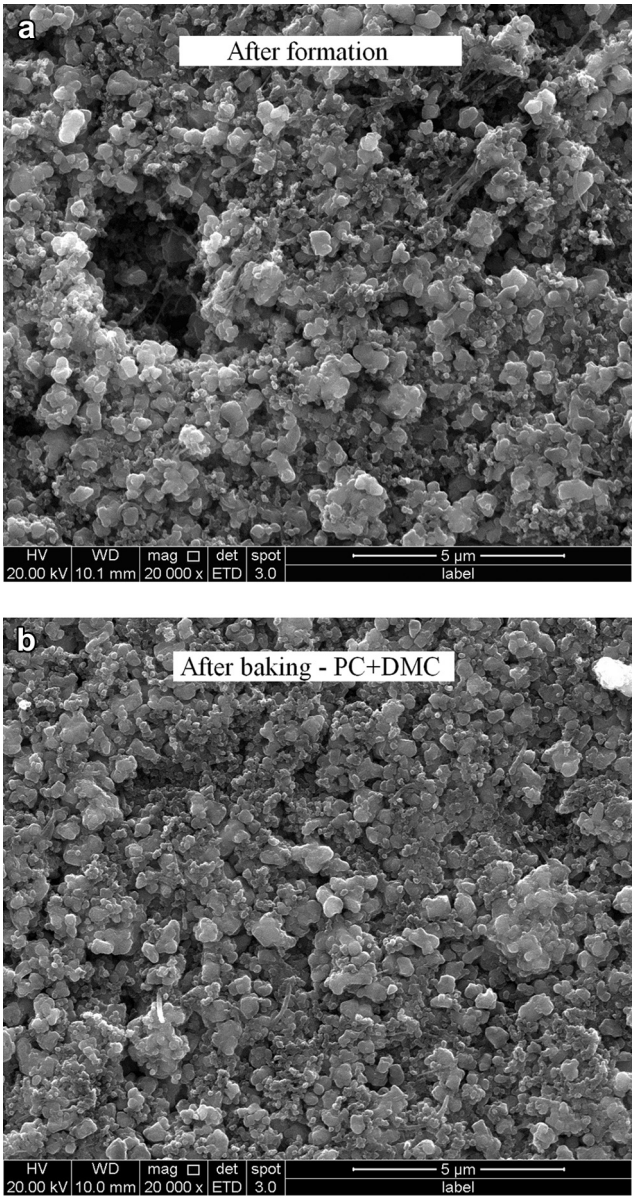

Fig. 6. SEM pictures of LTO electrodes before and after baking in PC + DMC.

took a mole ratio of more than 50% when electrolytes contained 80% PC. It implied that H_2 was apt to be produced from linear carbonates.

The LTO electrodes after baking tests were characterized by XRD, SEM, IR and XPS. As shown in Fig. 5 and Fig. 6, after baking crystalline phases were still dominated by spinel LTO in different electrolytes and the particle morphology almost kept intact. These results indicate that the baking test did not lead to the structure collapse and morphology change of LTO material. The deposits of electrolyte decomposition on LTO electrodes were analyzed with IR. The IR spectroscopies of $L_4Ti_5O_{12}$ powder, PVdF and Li_2CO_3 were also plotted as a control in Fig. 7. Besides the signals of LTO and PVdF, new peaks at 1502 cm^{-1} and 1442 cm^{-1} were detected after formation (Fig. 7a). They were probably assigned to C═O asymmetric stretching of RCOOLi and CH_2 bending of $(CH_2OCO_2Li)_2$ respectively, or C–O stretching of Li_2CO_3 (1488 cm^{-1}, 1434 cm^{-1}). These stuffs could not be clearly identified due to the limited amount of decomposing products. After baking, the new vibrations could be attributed to $ROCO_2Li$ (1655 cm^{-1}, 1444 cm^{-1}, 1330 cm^{-1}, 1290 cm^{-1}), Li_2CO_3 (1502 cm^{-1}, 1444 cm^{-1}, 1091 cm^{-1}, 865 cm^{-1}) and RCO_2Li (1577 cm^{-1}, 1502 cm^{-1}). These components were confirmed as the inorganic components of SEI film on graphite electrode [14–18]. Fig. 7b showed the IR spectroscopies of LTO electrodes after baking tests in different electrolytes. IR did not detect any new species in DMC and DEC electrolytes besides PVdF

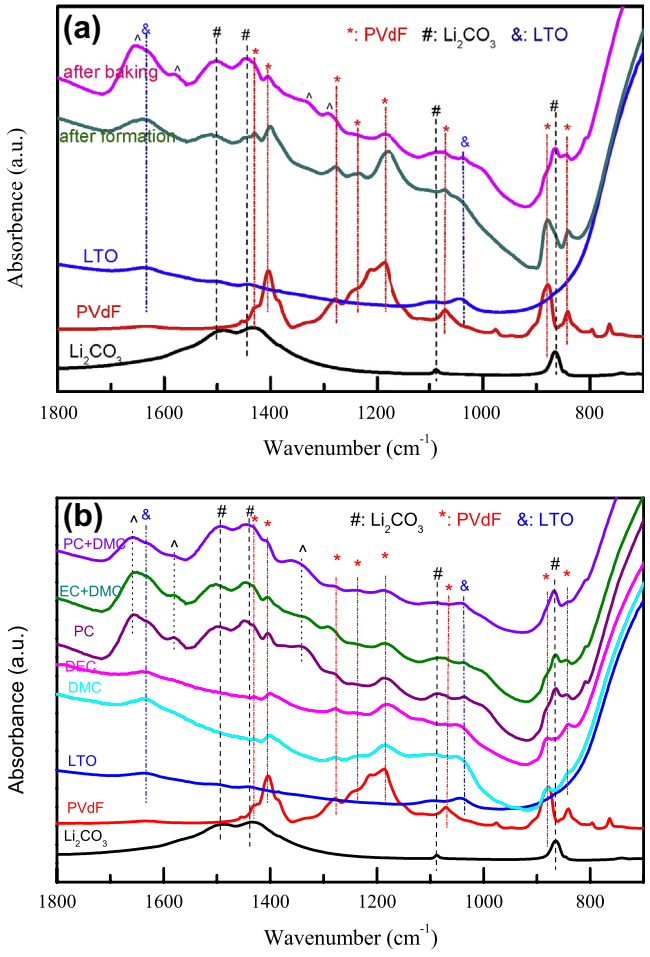

Fig. 7. IR spectroscopies of the LTO electrodes. a: after formation and after baking in 1 mol L^{-1} $LiPF_6$/EC + DMC; b: after baking in the different electrolytes. The IR spectroscopies of LTO, PVdF and Li_2CO_3 are also plotted as a control.

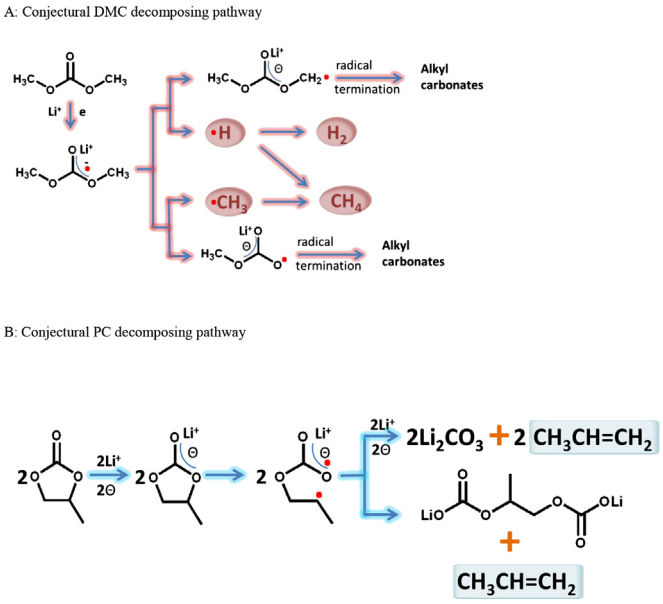

Scheme 1. Decomposition mechanism of DMC and PC.

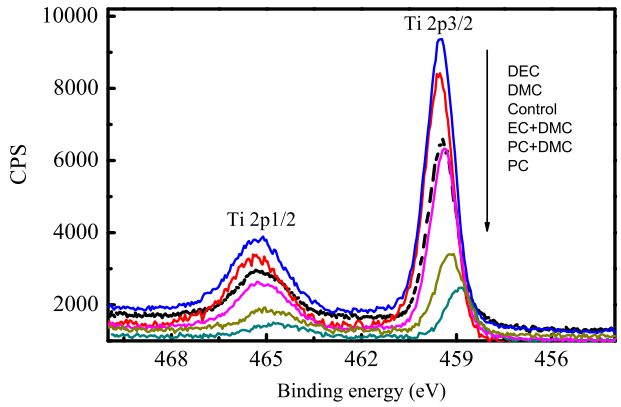

Fig. 8. XPS spectroscopies of the LTO electrodes in the investigated electrolytes. LTO electrode after formation in EC + DMC electrolyte is utilized as a control.

and $Li_4Ti_5O_{12}$. In the electrolytes containing cyclic carbonates, $ROCO_2Li$, Li_2CO_3 and RCO_2Li were identified as the remnants, which is similar to that in EC + DMC electrolyte.

According to the results of IR and GC, linear and cyclic carbonates should be decomposed by different reaction pathways. Linear carbonates seem to decompose to H_2, characteristic gas, and liquid species, while cyclic carbonates tend to produce alkene gas, Li_2CO_3 and dilithium alkyl carbonates. Their decomposing mechanisms are illustrated in Scheme 1 with DMC and PC as the example of linear/cyclic carbonates.

XPS was also utilized to analyze the surface characteristics of LTO electrodes. The electrode after formation in EC + DMC electrolyte was also tested as a control. As shown in Fig. 8, the intensities of titanium were stronger in both DEC and DMC electrolytes than those of the control and other electrolyte systems, indicating less surface deposits on these single solvent electrolytes. In contrast, the titanium signals in EC + DMC electrolyte were close to those of the control electrode, implying that baking does not result in more decomposition deposits in EC + DMC system. As for the electrodes in PC-based electrolytes, the titanium signals were seriously suppressed. It appears that PC-contained electrolyte can form the thicker/denser layer than EC-contained one on LTO surface.

Although single PC or DMC based electrolyte presented strong swelling effect, PC + DMC (1:1) electrolyte was able to suppress solvents decomposition more effectively. Combined with the results of cell swelling, XPS and IR analysis, we conjecture that a high-quality protective film could be formed in PC + DMC (1:1) electrolyte. The synergistic effect of both solvents for film formation is still under investigation in our labs. As for the difference between EC and PC based electrolytes, it could be attributed to the effect of steric hindrance of propylene group. Although no SEI formation was widely accepted as one of the advantage of LTO, to form the protective layer contained inorganic salts seemed to be the most effective remedy to lessen solvent's decomposition.

4. Summary

The mechanism of gas swelling in LTO cells has been investigated in this work. The inherent reason should be the electrochemical potential, instead of electrode moisture or others. As the reactants, electrolyte solvents underwent different decomposing pathways according to their structures. Linear carbonates mainly brought about H_2 and soluble species, and cyclic carbonates tended to produce alkylene gas and insoluble salts. Among the investigated systems, PC + DMC (1:1) electrolyte generated minimum gas as a result of the high quality of the protective layers. The cell swelling could be further diminished with the functional additives by forming stable protective film and/or absorbing radical groups.

Acknowledgment

The authors appreciate Amperex Technology Limited Com. (ATL) for the financial support. Dr. Deyu Wang and Mr. Chenyun Wang are obliged to Ningbo Key Innovation Team (grant no 2011B82005), 973 project (grant no 2012CB722704), and 100 Talents Program, Chinese Academy of Science.

References

[1] K.M. Colbow, J.R. Dahn, R.R. Haering, J. Power Sources 26 (1989) 397–402.
[2] E. Rossen, J.N. Reimers, J.R. Dahn, Solid State Ionics 62 (1993) 53–60.
[3] T. Ozuku, A. Aeda, Solid State Ionics 69 (1994) 201–211.
[4] T. Ozuku, A. Aeda, N. Yamamoto, J. Electrochem. Soc. 142 (1995) 1431–1435.
[5] K. Xu, A.V. Cresce, U. Lee, Langmuir 26 (2010) 11538–11543.
[6] I. Belharouak, G.M. Koenig Jr., K. Amine, J. Power Sources 196 (2011) 10344–10350.
[7] T.F. Yi, L.J. Jiang, J. Shu, C.B. Yue, R.S. Zhu, H.B. Qiao, J. Phys. Chem. Sol. 71 (2010) 1236–1242.
[8] K. Amine, I. Belharouak, Z. Chen, T. Tran, H. Yumoto, N. Ota, S.T. Myung, Y.K. Sun, Adv. Mater. 22 (2010) 3052–3057.
[9] K. Wu, J. Yang, Y. Zhang, C. Wang, D. Wang, J. Appl. Electrochem. 42 (2012) 989–995.
[10] I. Belharouak, G.M. Koenig Jr., T. Tan, H. Yumoto, N. Ota, K. Amine, J. Electrochem. Soc. 159 (2012) A1165–A1170.
[11] Y.B. He, B.H. Li, M. Liu, C. Zhang, W. Lv, C. Yang, J. Li, H.D. Du, B. Zhang, Q.H. Yang, J.K. Kim, F.Y. Kang, Scientific Rep. 2 (2012) 913.
[12] D. Aurbach, M. Daroux, P. Faguy, E. Yeager, J. Electroanal. Chem. 297 (1991) 225–244.
[13] G. Gachot, P. Ribiere, D. Mathiron, S. Grugeon, M. Armand, J.-B. Leriche, S. Pilard, S. Laruelle, Anal. Chem. 83 (2011) 478–485.
[14] P. Verma, P. Marie, P. Novak, Electrochim. Acta 55 (2010) 6332–6341.
[15] D. Aurbach, B. Markovsky, A. Shechter, Y. Ein-Eli, H. Cohen, J. Electrochem. Soc. 143 (1996) 3809–3820.
[16] Y. Ein-Eli, B. Markovsky, D. Aurbach, Y. Carmeli, H. Yamin, S. Luski, Electrochim. Acta 39 (1994) 2559–2569.
[17] A.N. Dey, B.P. Sullivan, J. Electrochem. Soc. 117 (1970) 222–224.
[18] D. Aurbach, M.L. Daroux, P.W. Faguy, E. Yeagur, J. Electrochem. Soc. 134 (1987) 1611–1620.